



MID-AMERICA TRANSPORTATION CENTER

Report # MATC-UNL: 101

Final Report



Foundation Design for High Tension Cable Guardrails

John Rohde, Ph.D., P.E.

Associate Professor

Midwest Roadside Safety Facility (MwRSF)

Nebraska Transportation Center

University of Nebraska-Lincoln

Ling Zhu, Ph.D.

Ryan J. Terpsma, B.S.M.E.



2010

A Cooperative Research Project sponsored by the
U.S. Department of Transportation Research and
Innovative Technology Administration

The contents of this report reflect the views of the authors, who are responsible for the facts and the accuracy of the information presented herein. This document is disseminated under the sponsorship of the Department of Transportation University Transportation Centers Program, in the interest of information exchange.
The U.S. Government assumes no liability for the contents or use thereof.

MATC

Foundation Design for High Tension Cable Guardrails

Submitted by

Ling Zhu, Ph.D.
Former Graduate Research Assistant

John R. Rohde, Ph.D., P.E.
Associate Professor

Ryan J. Terpsma, B.S.M.E.
Graduate Research Assistant

Midwest Roadside Safety Facility
University of Nebraska-Lincoln
130 Whittier Building
Lincoln, Nebraska 68588-0853
(402) 472-0965

Submitted to

Mid-America Transportation Center
262 Whittier Building
Lincoln, Nebraska 68588-0853

MwRSF Research Report No. TRP-03-236-10

June 2010

1. Report No. TRP-03-236-10		2.		3. Recipient's Accession No.	
4. Title and Subtitle Foundation Design for High Tension Cable Guardrails				5. Report Date June 2010	
				6.	
7. Author(s) Ling Zhu, John Rohde				8. Performing Organization Report No. TRP-03-236-10	
9. Performing Organization Name and Address Midwest Roadside Safety Facility (MwRSF) University of Nebraska-Lincoln 130 Whittier Building Lincoln, Nebraska 68588-0853				10. Project/Task/Work Unit No.	
				11. Contract © or Grant (G) No.	
12. Sponsoring Organization Name and Address Larry Rilett, Ph.D., PE Mid-America Transportation Center P.O. Box 830851 Lincoln, NE 68583-0851				13. Type of Report and Period Covered Final Report: 2009-2010	
				14. Sponsoring Agency Code MATC TRB RiP No. 17136	
15. Supplementary Notes					
16. Abstract (Limit: 200 words) <p>High tension cable guardrail is becoming increasing popular in median and roadside applications due to the promise of reduced deflections upon impact and reduced maintenance. As the performance of these systems is observed in service, there is a growing concern over the end anchorage foundation performance of current systems. Foundations for high tension systems must not only be capable of restraining the impact load of a vehicle but must also restrain the initial pretension on the cable system as well as temperature induced loads. While it may be acceptable for many roadside safety devices to require foundation repair after impact, foundation failure due to environmentally induced loads would be a serious maintenance problem. As initial tension and temperature induced loads can be greater than those loads applied during impact, this type of loading must be considered in foundation design. Foundation deflection can reduce cable tension, increasing deflection of the system during impact and letting the cables sag after impact. The soil conditions in which these foundations are placed vary significantly. This report considers the potential impact, tension, and temperature loads and develops a set of suggested foundation designs to accommodate a range of in situ soil conditions. These designs will vary significantly in different areas around the nation due to variations in both weather and in situ soil conditions. Deflection during full-scale crash tests may not accurately represent the foundation deflection that will be experienced in the field.</p>					
17. Document Analysis/Descriptors Roadside Safety, High tension Cable Barrier, Anchorage, Crash Testing, BARRIER VII simulation, LPILE simulation				18. Availability Statement No restrictions.	
19. Security Class (this report) Unclassified		20. Security Class (this page) Unclassified		21. No. of Pages 40	22. Price

Table of Contents

	Page
Technical Report Documentation Page	ii
Table of Contents	iii
List of Figures	v
List of Tables	vi
Chapter 1 Introduction	1
1.1 Problem Statement	1
1.2 Objective	2
1.3 Research Scope	2
Chapter 2 Thermal Effects on Cable.....	4
2.1 Thermal Load Change on a Fixed Length Cable	4
2.2 Thermal Deflection with Constant Cable Tension.....	6
2.3 Summary and Conclusions	6
Chapter 3 BARRIER VII Analysis	11
3.1 BARRIER VII Model	11
3.2 BARRIER VII Model Validation	11
3.3 BARRIER VII Analysis.....	14
3.4 Determination of Acceptable Anchorage Movement	15
Chapter 4 Evaluation of Alternate Cable Anchor Designs	17
4.1 Anchor Alternatives	17
4.2 Bogie Test	17
4.3 Conclusion	21
Chapter 5 LPILE Analysis	22
5.1 Problem Statement	22
5.2 LPILE Software Introduction	22
5.3 LPILE Plus Model Validation	24
5.3.1 <i>H-Pile Geometry Size Input</i>	24
5.3.2 <i>Soil Input</i>	26
5.3.3 <i>LPILE Plus Simulation Result</i>	27
5.4 LPILE Plus Analysis of Concrete Shaft Anchor Design	28
5.4.1 <i>Anchor Deflection in 350 Soil</i>	30
5.4.2 <i>Anchor Deflection in Stiff Clay Soil</i>	32
5.4.3 <i>Anchor Deflection in AASHTO A3 Sand</i>	34
5.5 Summary and Conclusion	36
Chapter 6 Conclusions	37

References..... 39

List of Figures

	Page
Figure 1.1 Brifen High tension Wire Rope Safety Fence (TL-4)	2
Figure 2.1 Illustration of Baseline Structure for Thermal Load Analysis	5
Figure 2.2 Thermal Load in Fixed Length Cable	5
Figure 2.3 Tension-Deflection Curves of Cable under Different Temperatures	8
Figure 2.4 Illustration of the Baseline Structure for Thermal Deflection Analysis	9
Figure 2.5 Thermal Deflections in Cables	10
Figure 3.1 Vehicle-Cable Impact of Test 4CMB-1	12
Figure 3.2 Validation of B7 Model with Full-Scale 4CMB-1	13
Figure 3.3 Effect of Per-Cable Tension on Maximum Lateral Deflection-MwRSF HT Model... ..	15
Figure 3.4 Cable Length Change vs. Cable Tension Change	16
Figure 4.1 Cable Anchor Bogie Test Setup	17
Figure 4.2 Three Anchor Designs	19
Figure 4.3 Force-Deflection Curves, Bogie Test CA-1, CA-3, and CA-4.....	20
Figure 5.1 Illustration of LPILE Plus Model	23
Figure 5.2 Test Setup of NYBBT-4 Soil Static Test	24
Figure 5.3 Illustration of H-Pile Movement Assumption in Soil.....	25
Figure 5.4 Comparison of Static Load Test Results and LPILE Plus Simulation	27
Figure 5.5 Illustration of External Force on Anchor Head	29
Figure 5.6 Illustration of LPILE Plus Model Setup.....	29
Figure 5.7 Boundary Condition Input in LPILE Plus	30
Figure 5.8 NCNRP 350 Soil Model Input Parameters in LPILE Plus.....	30
Figure 5.9 Concrete Shaft Head Deflection vs. Embedment Depth in NCHRP 350 Soil	31
Figure 5.10 Close-Up View of Concrete Shaft Head Deflection vs. Embedment Depth in NCHRP 350 Soil.....	32
Figure 5.11 Stiff Clay Soil Model Input Parameters in LPILE Plus	33
Figure 5.12 Concrete Shaft Head Deflection vs. Embedment Depth in Stiff Clay	33
Figure 5.13 Granular Rock Model Input Parameters in LPILE Plus.....	35
Figure 5.14 Concrete Shaft Head Deflection vs. Embedment Depth in Granular Rock	35

List of Tables

	Page
Table 1. Cable Thermal Length Change at Constant Tension	9
Table 2. Embedded Soil Type Options in LPILE Plus	23
Table 3. NYBBT-4 LPILE Plus Model Input-H-Pile Geometry	26
Table 4. Suggested K values for Sands in LPILE Plus.....	27
Table 5. Failure Embedment Depths of Concrete Shaft in NCHRP 350 Soil	31
Table 6. Failure Embedment Depths of Concrete Shaft in Stiff Clay	34
Table 7. Critical Embedment Depths of Concrete Shaft in Stiff Clay.....	34
Table 8. Failure Embedment Depths of Concrete Shaft in Granular Rock	35
Table 9. Critical Embedment Depths of Concrete Shaft in Granular Rock.....	36
Table 10. Recommended Embedment for Cylindrical Concrete Foundation.....	38

Disclaimer Statement

This report was funded in part through funding from the Federal Highway Administration, U.S. Department of Transportation. The contents of this report reflect the views and opinions of the authors who are responsible for the facts and the accuracy of the data presented herein. The contents do not necessarily reflect the official views or policies of the state highway departments participating in the Midwest States Regional Pooled Fund Program nor the Federal Highway Administration, U.S. Department of Transportation. This report does not constitute a standard, specification, regulation, product endorsement, or an endorsement of manufacturers.

Acknowledgements

The authors wish to acknowledge several sources that made a contribution to this project: The Midwest States' Regional Pooled Fund Program funded by the California Department of Transportation, Connecticut Department of Transportation, Illinois Department of Transportation, Iowa Department of Transportation, Kansas Department of Transportation, Minnesota Department of Transportation, Missouri Department of Transportation, Nebraska Department of Roads, New Jersey Department of Transportation, Ohio Department of Transportation, South Dakota Department of Transportation, Wisconsin Department of Transportation, and Wyoming Department of Transportation for participating in project and MwRSF personnel for constructing the barriers and conducting the crash tests.

Acknowledgment is also given to the following individuals who made a contribution to the completion of this research project.

Midwest Roadside Safety Facility

D.L. Sicking, Ph.D., P.E., Professor and MwRSF Director
J.D. Reid, Ph.D., Professor
R.K. Faller, Ph.D., P.E., Research Assistant Professor
R.W. Bielenberg, M.S.M.E., E.I.T., Research Associate Engineer
J.C. Holloway, M.S.C.E., E.I.T., Research Manager
K.A. Polivka, M.S.M.E., E.I.T., Research Associate Engineer
C.L. Meyer, B.S.M.E., E.I.T., Research Engineer II
A.T. Russell, B.S.B.A., Laboratory Mechanic II
K.L. Krenk, B.S.M.A, Field Operations Manager
Tom McMaster, Laboratory Mechanic I
Undergraduate and Graduate Assistants

Chapter 1 Introduction

1.1 Problem Statement

High tension cable guardrail is becoming increasingly popular in median and roadside applications due to the promise of reduced deflections upon impact and reduced maintenance. These systems show better performance in redirecting vehicles and preventing median crossovers than traditional low-tension cable guardrail systems. These high tension systems have also been shown to be more easily repairable with the undamaged lengths functioning properly throughout the repair process. As the performance of these systems is observed in service, there is a growing concern over the end anchorage foundation performance of current systems. Foundations for high tension systems must not only be capable of restraining the impact load of a vehicle, but must also restrain the initial pretension on the cable system as well as temperature induced loads. While it may be acceptable for many roadside safety devices to require foundation repair after impact, foundation failure due to environmentally induced loads would be a serious maintenance problem. As temperature induced loads can be greater than those loads applied during impact, these loadings must be considered in foundation design. Foundation deflection can reduce cable tension, increasing deflection of the system during impact and letting the cables sag after impact. The soil conditions in which these foundations are placed vary significantly. A soil specific foundation design would assure the functionality of these high tension systems.



Figure 1.1 Brifen High tension Wire Rope Safety Fence (TL-4)

1.2 Objective

The objective of this project is to assess foundation alternatives based on a selected suite of potential in situ soils to provide states with a rational, cost effective basis for specifying foundations in these critical barrier systems.

1.3 Research Scope

A literature research was conducted first. Analyses were then performed to investigate the thermal effects on the changes in cable tension, cable length, and foundation loads. The computer software Barrier VII was used to run simulations to evaluate the effect of foundation deflection on pre-tension and ultimately the high tension cable's redirecting capability. Further investigations were made into the effects of cable's tension change on the high tension cable's maximum lateral deflection during impact, and to determine the acceptable range of the anchorage's deflection.

An ideal anchorage design is desired to limit its deflection within a certain acceptable range throughout the year-round temperature fluctuations with minimum construction cost. Previous bogie tests conducted by MwRSF were reviewed to evaluate the existing common anchorage types and choose a proper design. The computer software LPILE was then used to evaluate the different anchorage designs in different soil conditions and to evaluate their foundation deflection in each respective soil. Three soil types were selected to represent soil conditions in various geographic regions: 350 soil (stiff), clay (medium), and sand (soft).

Finally, a guideline was developed for proper anchorage design in different soil types to resist the thermal expansion/contraction effect and maintain the high tension cable system's performance. A summarized version of the findings presented in this report was also submitted to the Transportation Research Board (1).

Chapter 2 Thermal Effects on Cable

The contraction of the cable due to a drop in temperature can generate significant load on the end anchorage, which may cause permanent deflection in the foundations, thus reducing cable tension and potentially affecting the high tension cable's performance. The impact of these thermal loads will be especially significant during seasons where soil stiffness is reduced by high moisture content.

Analyses were performed herein to investigate the thermal effects on cable structure. Two extreme scenarios were investigated—Extreme Stiff Anchorage, and Extreme Weak Anchorage—covering cable tension changes on a fixed length cable and cable length change on a free end cable, respectively.

2.1 Thermal Load Change on a Fixed Length Cable

If it is assumed that the foundation is infinitely stiff, the thermal load change in the cable can be calculated using Eq. 1—this load is independent of the cable's original length. Assuming the cable's design tension is 4,200 lb at 110 F, the tensile load in the cable versus temperature is shown in Figure 2.2, the cable tension can reach up to 7,000 lb when the temperature drops to -20 F. Thus, for the 4-cable barrier, the load on the anchor caused by the temperature could be as high as 28 kips. Also, it was concluded from Eq. 1 that the thermal load change depends on the cable structures' cross sectional area, and is independent of the cable's original length. Thus, for various cable installation lengths, the thermal loads on the end anchors are the same.

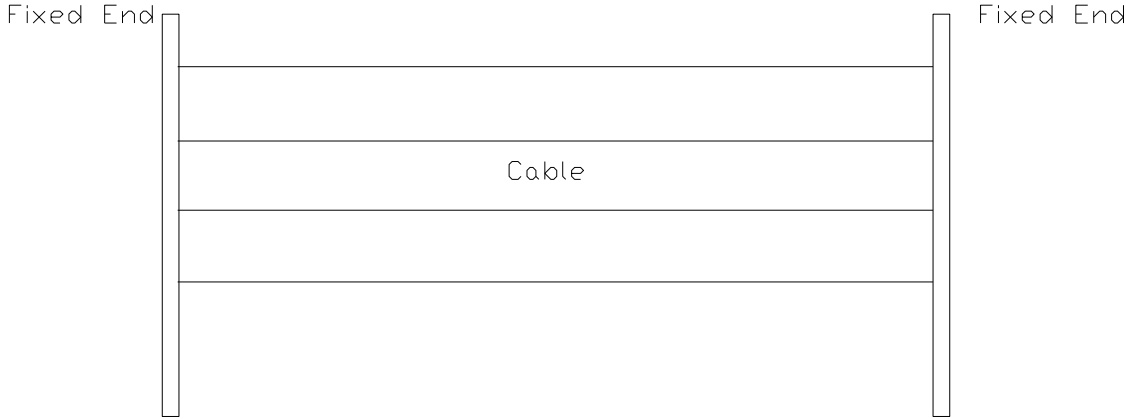


Figure 2.1 Illustration of Baseline Structure for Thermal Load Analysis

$$\Delta F = A * E * \alpha * \Delta T$$

Eq. 1

- A*: Cable Cross Section Area
- E*: Cable Material Young's Modulus
- α*: Thermal Expansion Coefficient
- ΔT*: Temperature Change

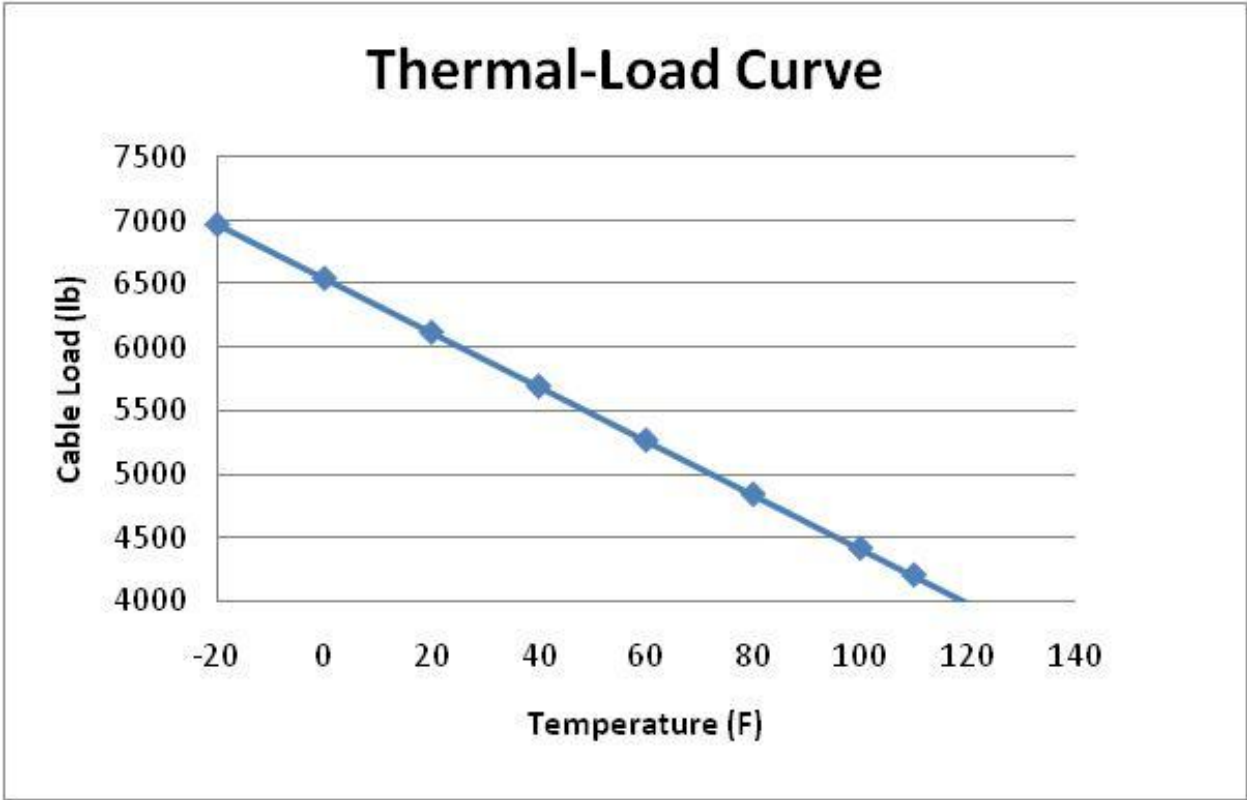


Figure 2.2 Thermal Load in Fixed Length Cable

2.2 Thermal Deflection with Constant Cable Tension

For a weak anchor design, the cable's actual length contracts when the ambient temperature drops. The thermal effect on the cable length change was investigated herein, assuming the end anchors are extremely weak and the cable can freely contract when the temperature changes.

A cable was fixed at one end, and the other end was allowed to extend and contract freely due to temperature change, as shown in Figure 2.4. Based on Eq. 2, calculations were performed to determine the cable length change due to temperature change. Since the length change is related to the cable's original length, four different length cables were analyzed: 1 mile, ½ mile, ¼ mile, and 1/8 mile. The baseline temperature was 110 F.

Nine different temperature points were calculated, ranging from -20 F to 120 F. Corresponding results are shown in Figure 2.5 and Table 2.1, and indicate that, for a one-mile cable system, the cable can contract as much as 50 inches due to the temperature change if the anchor is not properly designed.

$$\Delta L = \alpha * L * \Delta T$$

Eq. 2

L: Cable Original Length

α: Thermal Expansion Coefficient

ΔT: Temperature Change:

ΔL: Cable Length Change

2.3 Summary and Conclusions

From this analysis, shown in Figure 2.2, it is clear that the change of temperature can have a significant effect on the cable tension. For a cable system built with a designed tension of 4,200 lb at the temperature of 110 F, when the ambient temperature drops to -20 F, each cable can have an extra 2,800 lb force, which is 66% more than its original designed load. Since a

single cable will not yield until 28,000 psi, this temperature fluctuation is not going to cause yielding, and the analysis conducted with the assumption of elastic behavior is valid.

Meanwhile, the temperature change can result in cable length change and move the end anchors if the anchors are not properly designed. The length change is related to the cable's original length, and for a one mile long cable, the length change can be as much as 50 in. due to temperature fluctuations.

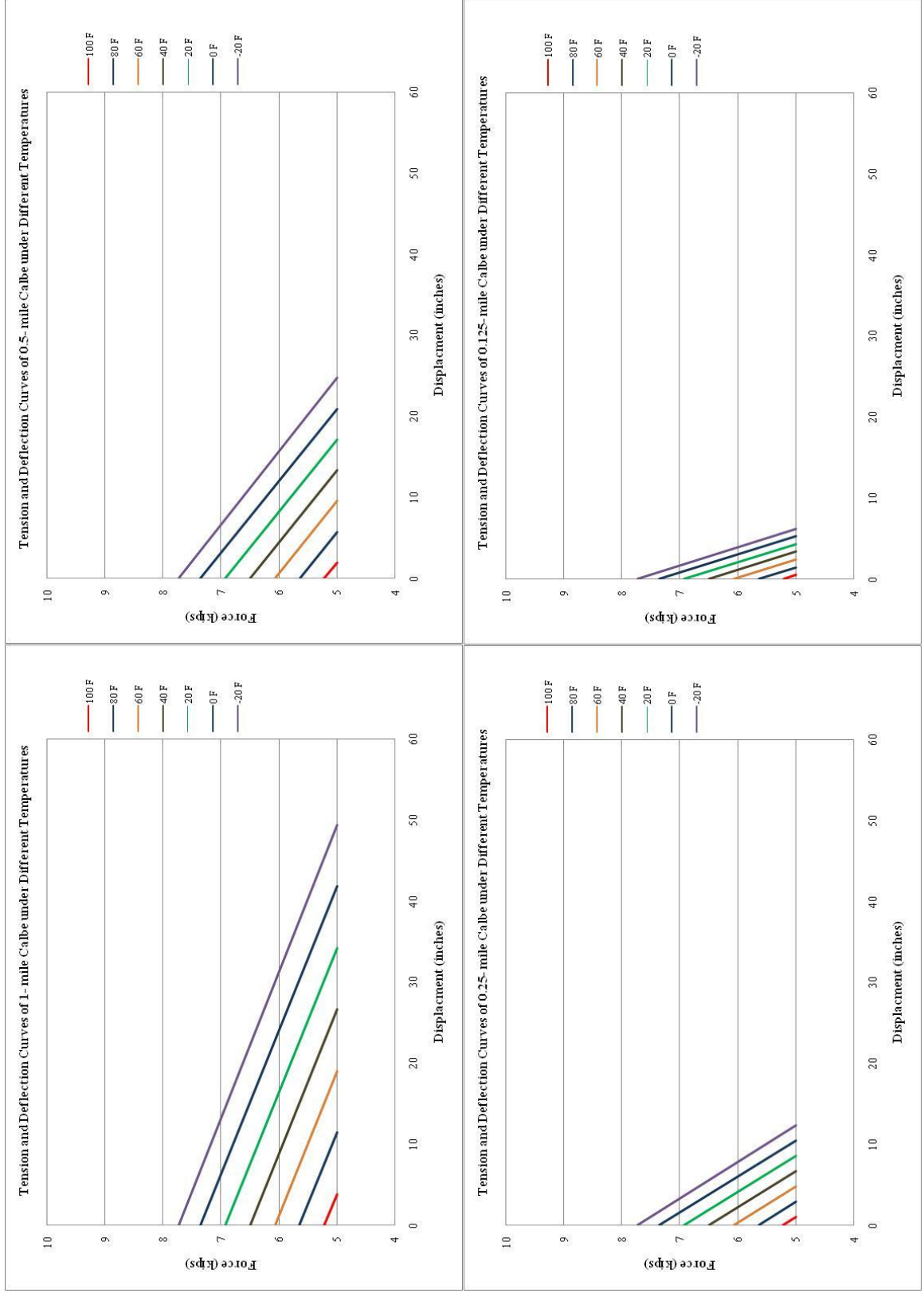


Figure 2.3 Tension-Deflection Curves of Cable under Different Temperatures

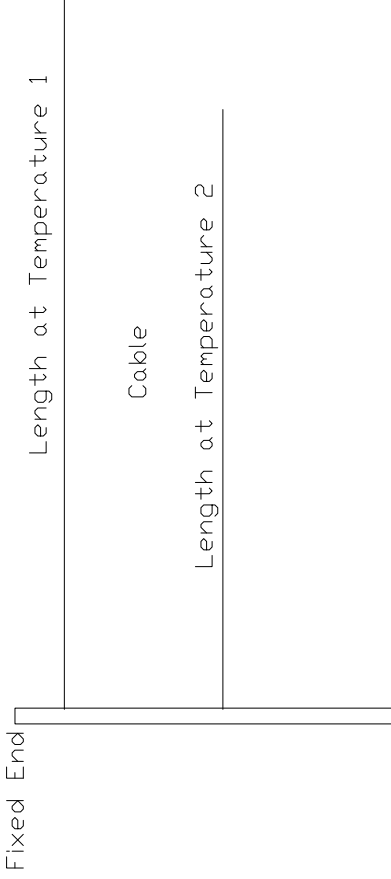
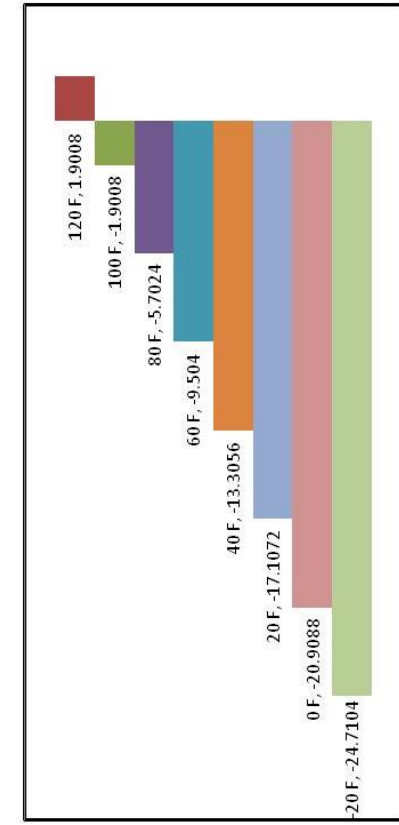


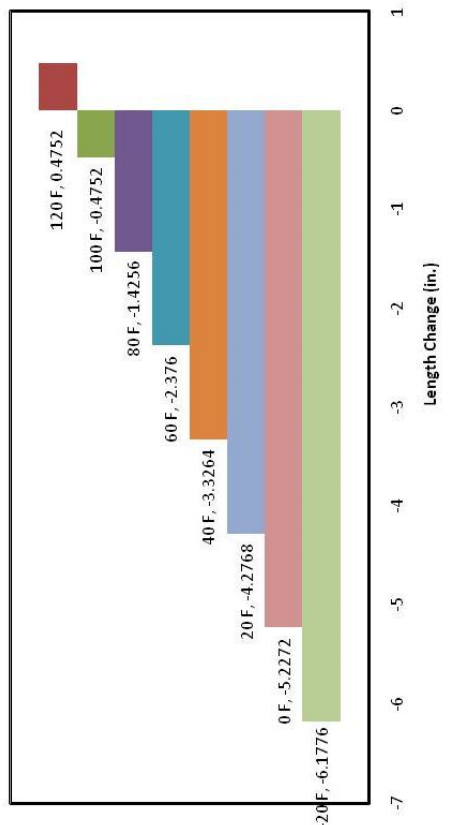
Figure 2.4 Illustration of the Baseline Structure for Thermal Deflection Analysis

Table 2.1 Cable Thermal Length Change at Constant Tension

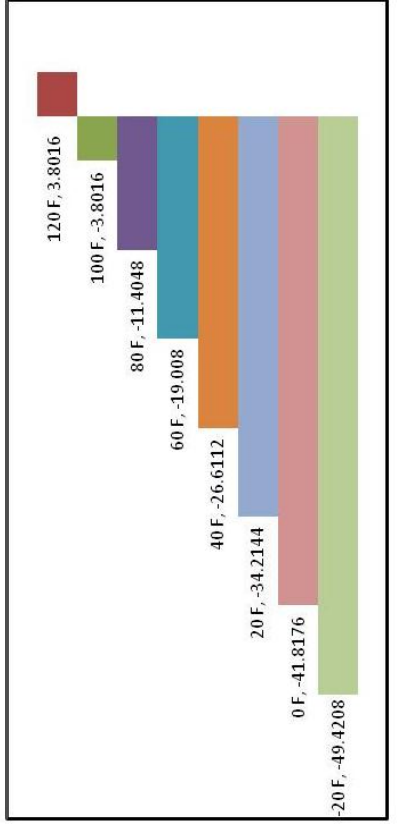
	120	110	100	80	60	40	20	0	-20	
Cable	Initial 1 Mile	3.8016	0	-3.8016	-11.4048	-19.008	-26.6112	-34.2144	-41.8176	-49.4208
Length	Initial 0.5 Mile	1.9008	0	-1.9008	-5.7024	-9.504	-13.3056	-17.1072	-20.9088	-24.7104
Change	Initial 0.25 Mile	0.9504	0	-0.9504	-2.8512	-4.752	-6.6528	-8.5536	-10.4544	-12.3552
(in.)	Initial 0.125 Mile	0.4725	0	-0.4752	-1.4256	-2.376	-3.3264	-4.2768	-5.2272	-6.1776



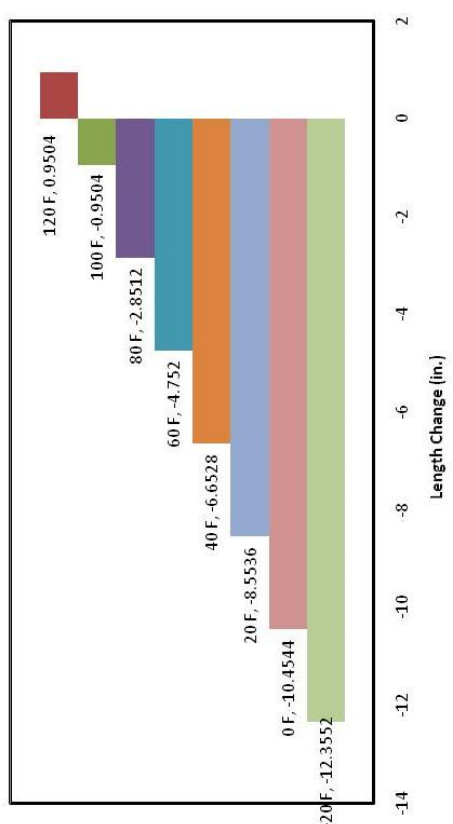
1/2-Mile Cable Length Change



1/8 Mile Cable Length Change



1-Mile Cable Length Change



1/4 Mile Cable Length Change

Figure 2.5 Thermal Deflections in Cables

Chapter 3 BARRIER VII Analysis

A significant advantage of high tension cable systems is believed to be the reduced amount of lateral deflection during impact as compared to a low-tension system. As previously discussed, inadequate anchorage designs might be compromised by temperature induced loads. Subsequent cable tension will be reduced by the anchorage movement, which will increase the lateral impact deflection and compromise the cable's redirecting ability. In order to quantify the cable's tension effect on its lateral deflection during impact, BARRIER VII simulation was used to predict the dynamic performance of high tension cable system under different cable tensions. This analysis consisted of a calibration process and a tension-deflection analysis.

3.1 BARRIER VII Model

To evaluate the impact of loss in cable tension associated with anchor deflection, a series of BARRIER VII simulations were performed to assess working width changes in the system. The model has a length of 606 ft with a line post spacing of 16 ft. The two ends of the cable system were simplified with one end post on each end. Due to the limitations of BARRIER VII, only two cables can be modeled despite the fact that there are 4 cables in the actual system. The choice of cables depended on the particular impact case. The two cables that were perceived to carry most of the load from the impact in the previous full scale crash test were chosen for the BARRIER-VII model.

3.2 BARRIER VII Model Validation

In the test of 4CMB-1, a 2270P pickup truck ran off a ditch and impacted the cable at the point at 3 ft downstream of Post no. 15, as shown in Figure 3.1. Since the major vehicle interaction occurred on the top two cables in test 4CMB-1, the two cable heights in the BARRIER VII model were set to 35 inches and 45 inches respectively. A baseline high tension

cable barrier model was built using BARRIER VII to replicate the previously conducted full-scale crash test 4CMB-1, the validation results are shown in Figure 3.2.

The 4CMB test series was used for the validation because they are the only full-scale tests that have been conducted on the MwRSF high tension cable system so far. However, BARRIER-VII is a 2-D program and can only model flat vehicle-barrier impacts. In order to minimize the discrepancy, 4CMB-1 was chosen for the validation since, of the three tests run, it exhibited the smallest diving angle.

The model was run with various cable pre-tensions and the cable's maximum lateral dynamic deflections for each of the pre-tension levels were recorded; the results are plotted in Figure 3.3. The impact of the increased lateral deflection on system design depends on the requirements for a given installation.



Figure 3.1 Vehicle-Cable Impact of Test 4CMB-1

The cable's dynamic deflection during impact is difficult to track during impact and, as such, is unavailable. Consequently, the trajectory data of the vehicle's C.G. acquired from the overhead high-speed film was used to calibrate the BARRIER VII simulation to the 4CMB-1 test. For the validation effort, several simulations were performed at the impact condition of the crash test in order to calibrate selected BARRIER VII input parameters.

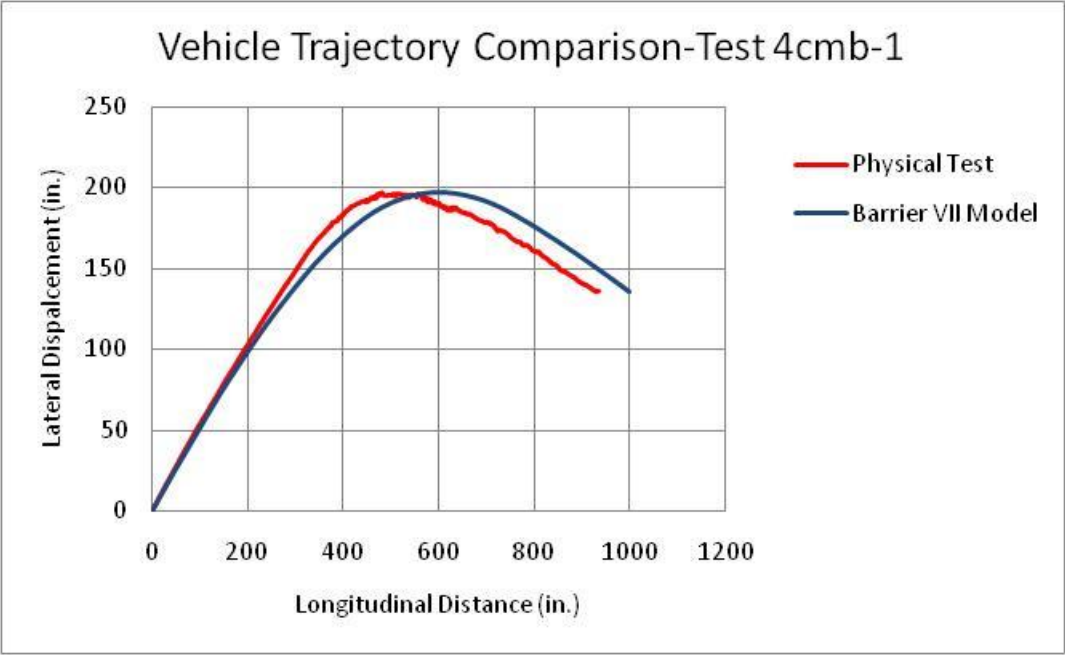


Figure 3.2 Validation of B7 Model with Full-Scale 4CMB-1

3.3 BARRIER VII Analysis

Once the calibration effort was completed for test 4CMB-1, simulations to investigate the cable's tension effect on its maximum lateral deflection during impact were initiated using the same parameters determined in the 4CMB-1 validation effort.

In the case of test no. 4CMB-1, the pickup truck came in contact with the top two cables due to the ditch. However, most vehicle-cable impacts occur on the two middle cables (2nd and 3rd) so in order to cover the most common pickup-cable impact scenarios, the cable heights in the BARRIER VII model were adjusted to 35 in. and 25 in. from the 45 in. and 35 in. heights used in the calibration model.

The baseline scenario was a 2270P pickup truck impacting the high tension cable barrier at a speed of 100 km/h (62 mph) and at an angle of 25 degrees. Ten various initial cable tensions from 0 psi to 10,000 psi at an equal interval were assigned to the high tension cable system. The maximum dynamic lateral deflection at each pre-tension level was recorded and plotted as in Figure 3.3.

As shown in Figure 3.3, the reduction of the cable's tension has a significant effect on the cable's maximum lateral deflection during redirection of errant vehicles. The maximum lateral cable deflection increases 4 inches for every 1,000-lb drop in cable pre-tension.

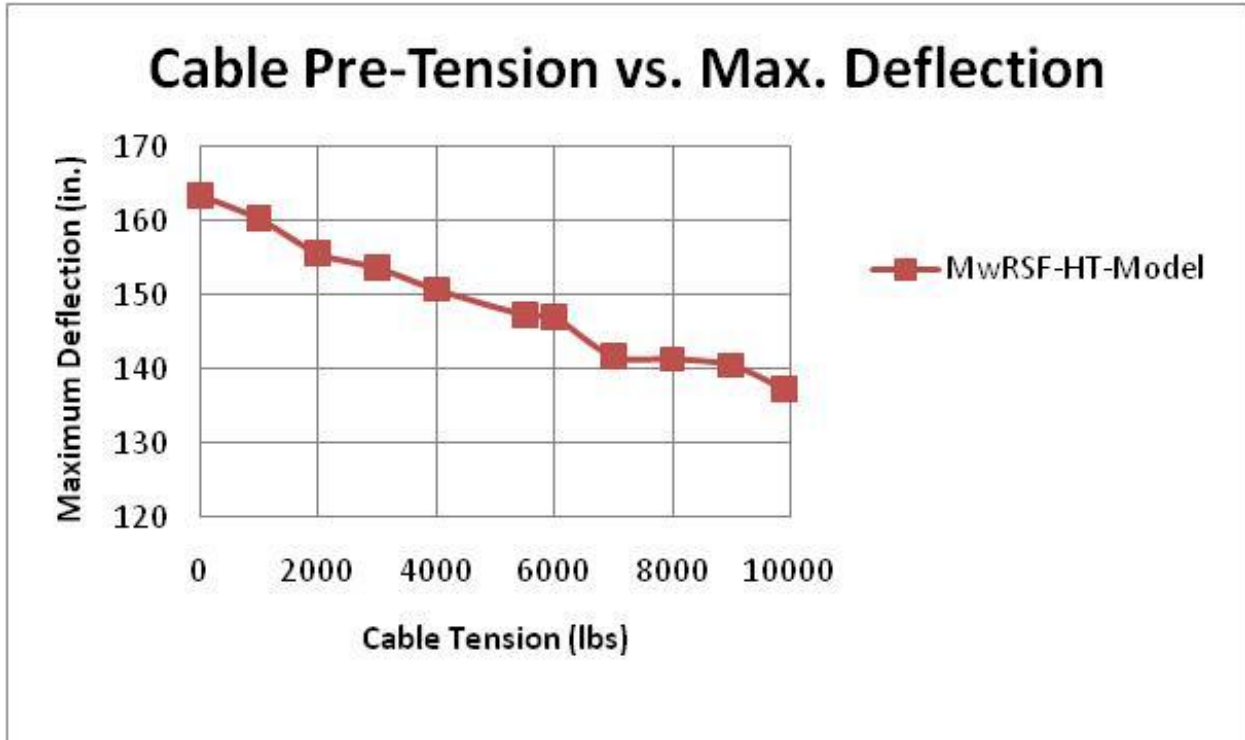


Figure 3.3 Effect of Per-Cable Tension on Maximum Lateral Deflection-MwRSF HT Model

3.4 Determination of Acceptable Anchorage Movement

A significant advantage of high tension cable systems is that its redirective capability is not always lost after an impact. With sufficient pretension the cable will still have sufficient tension to hang in the air after impact. Clearly, if sufficient anchor movement occurs, which reduces or negates pretension, this advantage will be lost.

In the section above, it was clearly demonstrated that the change in cable tension had a significant effect on the cable's redirecting performance. The loss of cable tension is nearly linear to the increase of cable's maximum lateral deflection. Since the tension loss is caused by the anchorage movement, the relationship between the anchorage movement and the cable lateral deflection can be determined.

$$T = E \cdot \Delta L \cdot A / L$$

Eq. 3

- T*: Cable Tension
- E*: Cable Young's Modulus
- ΔL : Cable Length Change
- A*: Cable Cross Section Area
- L*: Initial Cable Length

Characteristic of the most common 3x7 cable, the average Young's Modulus is around 15,500 ksi, and the cross sectional area is 0.24 in². To be consistent with the analysis in Chapter 2, four cable systems with different lengths are investigated: 1/8 mile, 1/4 mile, 1/2 mile, and 1 mile, and their results are shown in Figure 3.4.

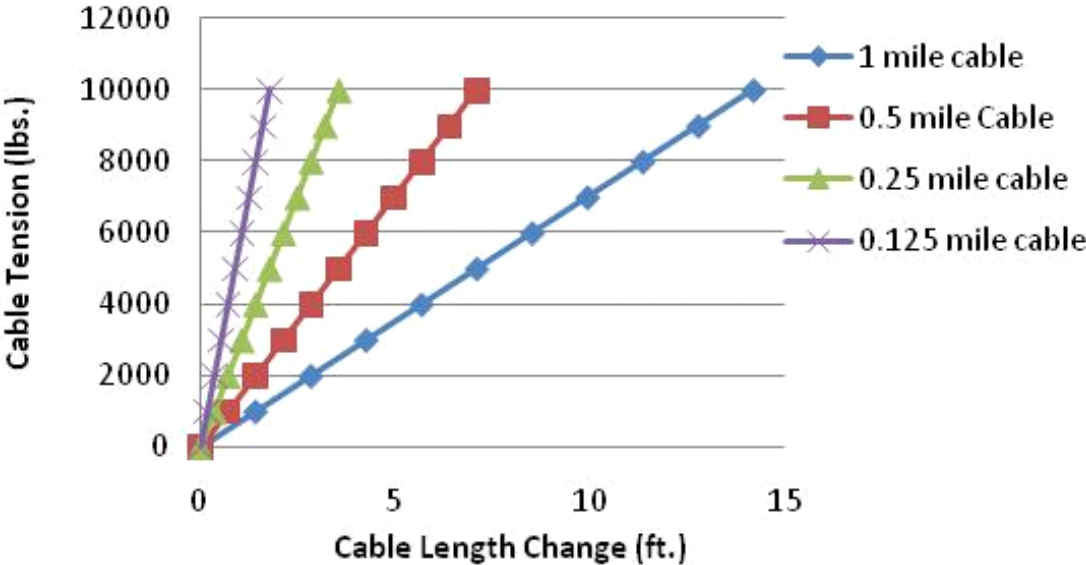


Figure 3.4 Cable Length Change vs. Cable Tension Change

Chapter 4 Evaluation of Alternate Cable Anchor Designs

4.1 Anchor Alternatives

Three different anchor design options were previously evaluated and tested by MwRSF, including a reinforced concrete block, a reinforced concrete shaft, and a driven steel post. The concrete block option mimics that of the old anchor designs. The reinforced concrete shaft provides a simplified concrete design alternative, but still relies on the use of cast-in-place concrete. The steel post design incorporates a large steel beam that is driven into the ground.

4.2 Bogie Test

In 2000, Midwest performed a series of bogie tests on 3 anchor designs: steel H-pile, concrete shaft, and concrete block, as shown in Figure 4.1 and Figure 4.2. All the three anchor designs were buried in the ground and were pulled by a 4,900-lb bogie vehicle at a target speed to provide a minimum dynamic load of 40,000 lbs. A string potentiometer and high speed video were used to monitor anchor motions during the tests. The force-deflection curves of each test are plotted in Figure 4.3.

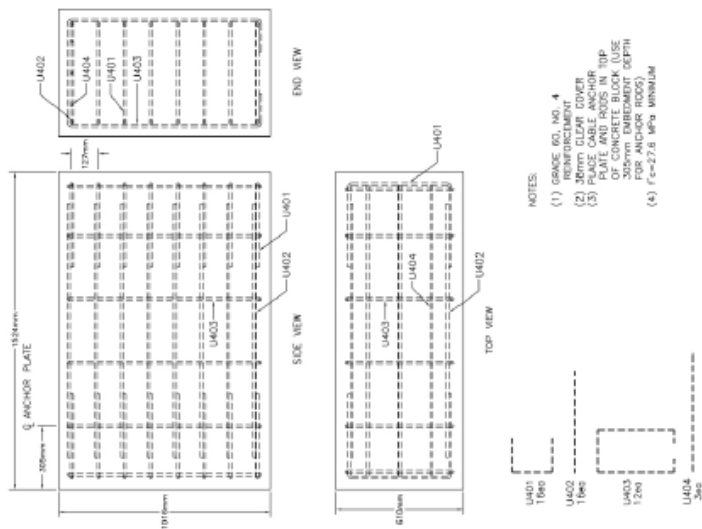


Figure 4.1 Cable Anchor Bogie Test Setup

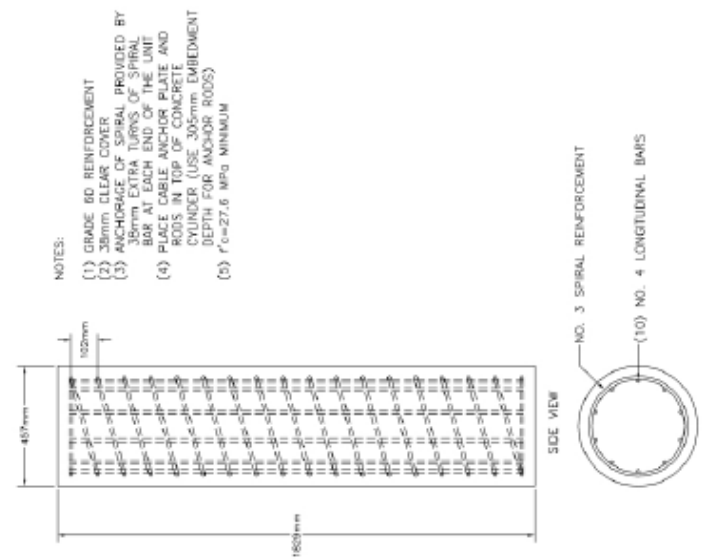
In test CA No. 1, a W6x25 steel section with 36 ksi yield strength and a 96 in. overall length was selected for the anchor design. The addition of a 24 x 24 x ½ in. soil bearing plate provides further resistance against lateral force, as shown in the diagram on the left side of Figure 4.2.

In test CA No.3, a concrete shaft with an 18 in. diameter and 72 in. total length was used as the anchor design. The anchor was reinforced with a spiral rebar cage fabricated with Grade 60 steel. The spiral reinforcement was designed with a 1.5 in. clear cover over No. 3 rebar and ten No. 4 vertical bars equally spaced around the interior circumference. A concrete mix with compressive strength of 4,000 psi was also specified. Anchor rods embedded 12 in. into the structure were used to secure the cable anchor bracket, as shown in the middle of Figure 4.2.

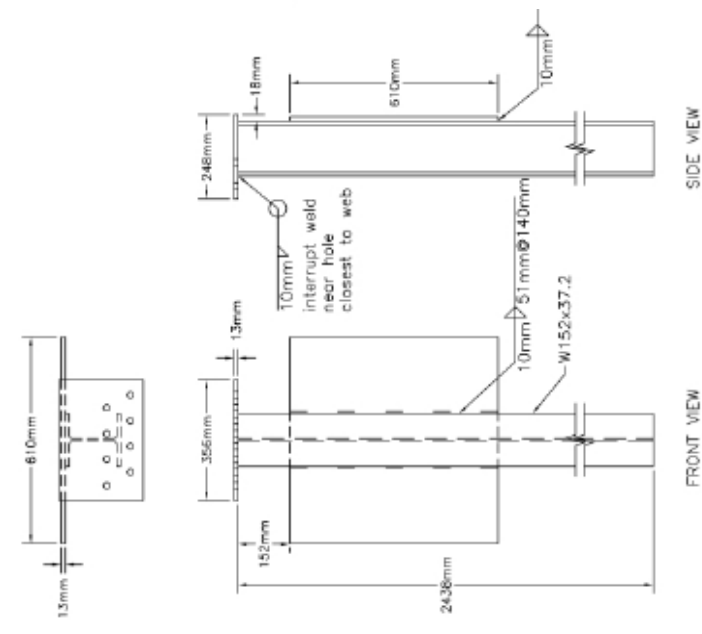
In test CA No. 4, a 60 x 40 x 24 in. concrete block, weighing approximately 5,000 lbs, was used as the anchor design. The block was fabricated using 4,000 psi minimum compressive strength concrete with No. 4 steel bars, Grade 60 for reinforcement, as shown in the right side of Figure 4.2.



Test CA-4 (Concrete Block)



Test CA-3 (Concrete Shaft)



Test CA-1 (Steel H-Pile)

Figure 4.2 Three Anchor Designs

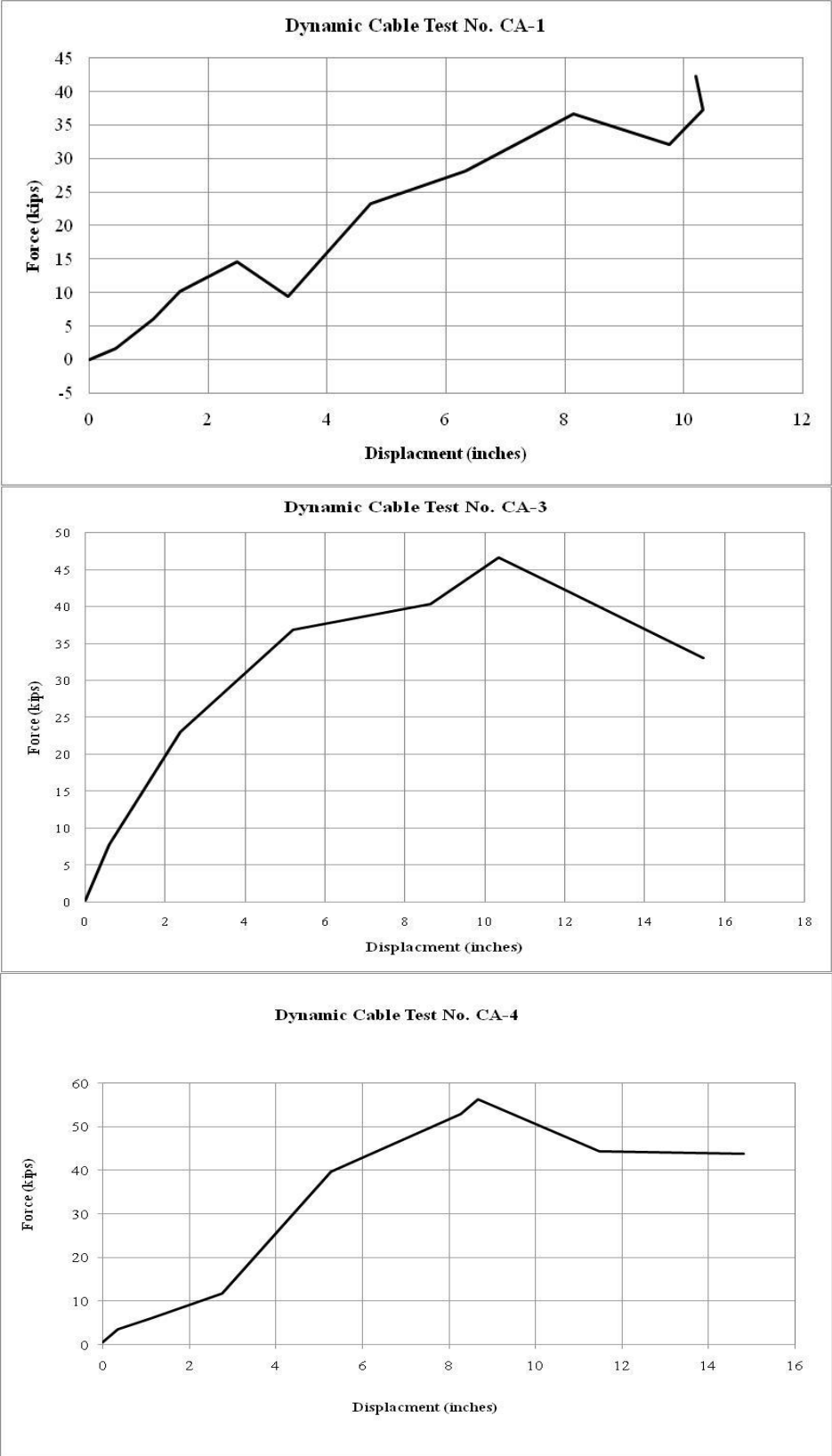


Figure 4.3 Force-Deflection Curves, Bogie Test CA-1, CA-3, and CA-4

4.3 Conclusion

The bogie test results are summarized by force-deflection curves, as shown in Fig 4.3. The reinforced concrete block option represented the strongest design and is characterized by a 254 kN (57-kip) peak resisting force. The drilled shaft produced a maximum lateral force equal to 205 kN (46 kips). The driven steel post proved to be the weakest anchor and sustained a 187 kN (42-kip) peak load. The results indicate that the minimum criterion set for the anchor force and displacement were met by the concrete shaft and concrete block anchor designs.

However, while the concrete block anchor utilizes the most material and is costly to construct, the drilled shaft concrete anchor provides a more economical alternative by reducing the volume of concrete and simplifying excavation. This design provides a simple alternative and utilizes equipment that is usually available on a guardrail construction site.

Considering the performance and cost, the concrete shaft anchor was determined to be the best option for this project. All of the analysis conducted utilized this anchor type.

Chapter 5 LPILE Analysis

5.1 Problem Statement

Based on the BARRIER VII analysis, the deflection of cable anchor will reduce the cable's tension and compromise its redirecting performance during vehicle impacts. To assure the high tension cable system's performance, an anchor's deflection under both static temperature and dynamic loads should be limited to assure adequate performance.

The lateral deflection of a relatively short pile foundation is affected by its diameter, embedment length and soil properties. Increases in diameter and/or depth increase lateral load capacity and decrease deflection. Optimization of foundation strength/stiffness versus cost must also consider construction equipment typically available on site and the expertise of the contractor. Most existing systems were tested under the requirements in the NCHRP 350 Report, meaning that the deflection of the foundations due to cable pretension and impact load are significantly less than may be anticipated with typical soils found along the roadside. To rationally design an anchor capable of reasonable deflections under temperature induced loads it is necessary to evaluate the anchor's performance in various soil types. Three soil types considered were: NCHRP 350 soil, stiff clay, and sand. These three soil types cover the typical range of in-situ soils across the nation.

5.2 LPILE Software Introduction

To evaluate the range of foundation diameters and embedment lengths required for varying soil conditions, a parameter study was conducted to evaluate each of their relative influences. The study was performed using LPILE, a widely accepted analysis program for evaluating laterally loaded piles. LPILE has been validated for various foundations evaluated at

MwRSF over the past several years and the confidence in modeling standard strong soil under NCHRP Report 350 is high.

Soil behavior is modeled with p-y curves internally generated by the computer program following published recommendations for various types of soils, and there are 10 embedded soil options in the LPILE Plus, as shown in Table 5.1. Alternatively, the user can manually introduce other p-y curves. Special procedures are programmed for developing p-y curves for layered soils and for rocks.

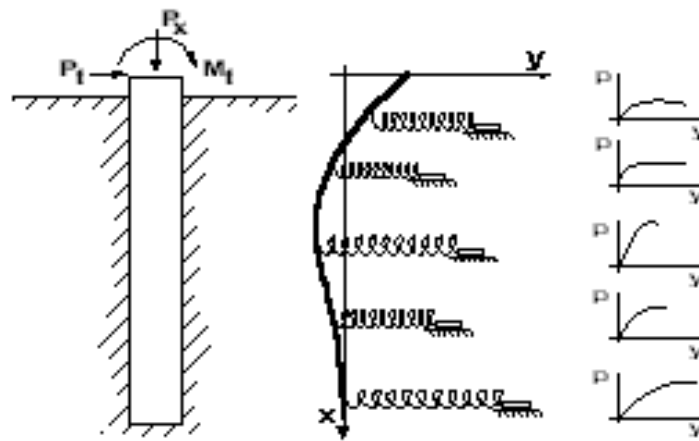


Figure 5.1 Illustration of LPILE Plus Model

Table 5.1 Embedded Soil Type Options in LPILE Plus

Number	1	2	3	4	5
Soil Type	Soft clay (matlock)	Stiff clay with free water (Reese)	Stiff clay without free water(Reese)	Sand (Reese)	Strong Rock (Vuggy Limestone)
Number	6	7	8	9	10
Soil Type	Silt (Cemented c-phi soil)	API Sand (O'Neil)	Week Rock (Reese)	Liquefiable Sand	Stiff Clay w/o free water using k

Several types of pile-head boundary conditions may be selected, and the properties of the pile can also vary as a function of depth. LPILE Plus has capabilities to compute the ultimate moment capacity of a pile's section and can provide design information for rebar arrangement.

The user may optionally ask the program to generate and take into account nonlinear values of flexural stiffness (EI) which are generated internally based on specified pile dimensions, material properties, and cracked/uncracked concrete behavior.

5.3 LPILE Plus Model Validation

A validation was first performed to determine the proper soil input parameters. Since LPILE Plus cannot replicate dynamic tests, a static physical test was used instead of the bogie tests above to validate the LPILE Plus model.

MwRSF previously performed a static soil test of New York Box Beam Terminal full-scale test (NYBBT-4). An I-shape structural steel beam (W6x16) was embedded 40 in. into the ground with a static load applied laterally at 25 in. above the ground line, as shown in Figure 5.2. An LPILE Plus model was then developed to replicate NYBBT-4 soil static test.

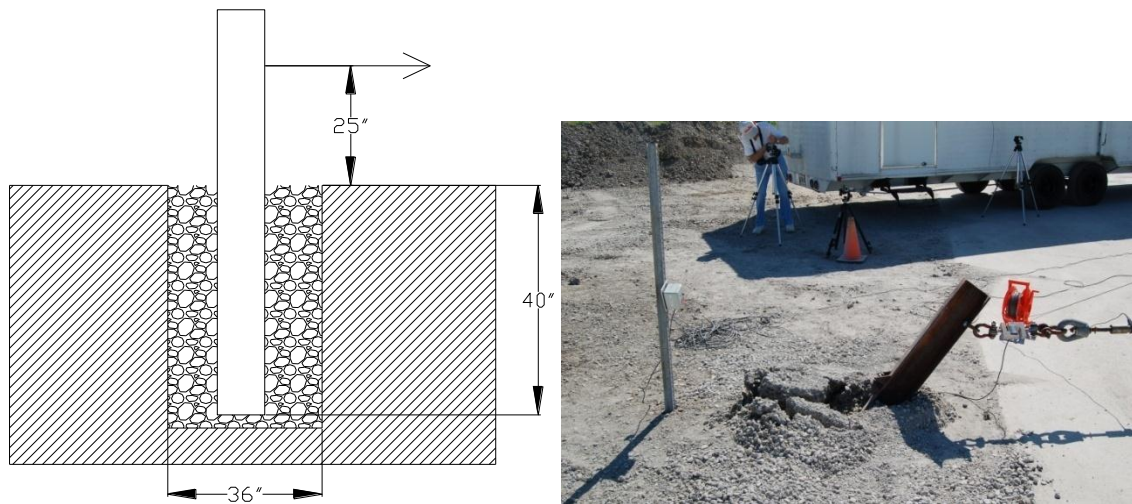


Figure 5.2 Test Setup of NYBBT-4 Soil Static Test

5.3.1 *H-Pile Geometry Size Input*

Because the recommendations for p-y curves are based strongly on the results of experiments with cylindrical shapes, all the piles in LPILE Plus are handled as circular cross-

section pile, and it requires the diameter for the pile property input. All the non-circular cross-section piles have to translate their cross-section geometric size into equivalent diameters (De).

For H-Pile it can be assumed that the soil in the flanges will move with the pile and that it will behave as a rectangular shape, as shown in Figure 5.3. Thus, the equivalent diameter (De) of the H-pile can be computed by finding a circular section with the same area as the rectangular section (2). Thus,

$$\pi De^2/4 = L \times H$$

Eq. 4

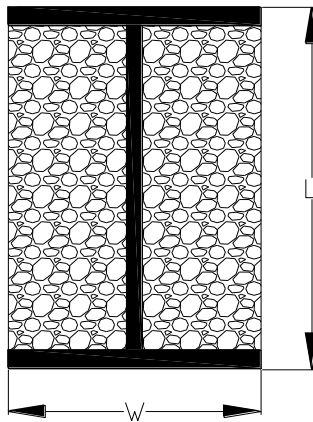


Figure 5.3 Illustration of H-Pile Movement Assumption in Soil

For the W6x25 H-pile used in the static test of NYBBT-4, the cross section depth (L) and width (W) are 6.38 in. and 6.08 in., respectively. Thus, the diameter input of a W6x25 H-pile was determined to be 7.03 in.

Table 5.2 NYBBT-4 LPILE Plus Model Input-H-Pile Geometry

Total Pile Length (in.)	40
Number of Increments	100
Distance from Pile Top to Ground Surface (in.)	0
Combined Ground Slope and Batter Angles (degrees)	0
Diameter (in.)	7.03
Moment of Inertia (in.^4)	53.4
Area (in.^2)	7.34
Modulus of Elasticity (lbs/in.^2)	29,000,000

5.3.2 Soil Input

As mentioned previously, there are ten soils templates embedded in LPILE Plus. Type 7 (API sand (O'Neil)) was determined to be close to NCHRP 350 soil. Three parameters are required for API sand option: *Density*, *Internal Friction Angle*, and *p-y modulus (k) value*. The density was determined from the test to be 0.08 lb/in³ and the friction angle was around 40 degrees.

The k value is the constant used in the equation $E_s = kx$. This constant is in units of force per cubic length and depends on the type of soil and lateral loading imposed to the pile group. It has two different uses: (1) to define the initial (maximum) value of E_s on internally-generated p-y curves of stiff clays with free water and/or sands, and (2) to initialize the E_s array for the first iteration of pile analysis.

Suggested values of the parameter k used for sands are given in Table 5.3. Since the 350 soil is a relatively dense soil, 225 (lb/in³) is a proper choice for the K value. Based on the

consideration that the K value of the 350 soil recommended by Dr. Rohde is $800 \text{ lb/in}^3 \pm 100 \text{ lb/in}^3$, four different K values (225, 700, 800, and 900) were run and compared in the simulation.

Table 5.3 Suggested K values for Sands in LPILE Plus

Relative Density	Loose	Medium	Dense
Submerged Sand	20 lb/in ³ 5,430 kPa/m	60 lb/in ³ 16,300 kPa/m	125 lb/in ³ 33,900 kPa/m
Sand Above Water Table	25 lb/in ³ 6,790 kPa/m	90 lb/in ³ 24,430 kPa/m	225 lb/in ³ 61,000 kPa/m

5.3.3 LPILE Plus Simulation Result

The H-Pile’s deflections vs. the lateral forces using different k-values from the LPILE simulation were plotted against the physical test data in Figure 5.4 As shown in this figure, the simulation replicated the physical test data the best when k value equaled 900.

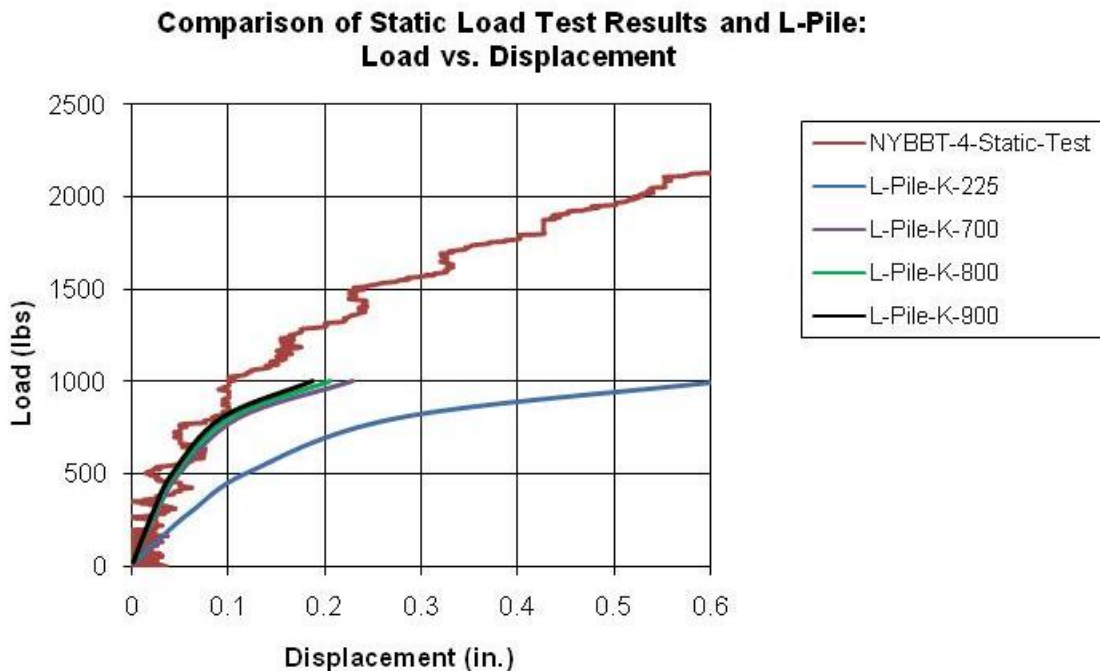


Figure 5.4 Comparison of Static Load Test Results and LPILE Plus Simulation

Though the LPILE Plus simulation presented good agreement with the physical static test, the maximum load from LPILE Plus simulation was only around 1,100 lbs. This value is close to the result calculated from Brom’s Equation (3), as shown in Eq. 5; while the maximum

load from the NYBBT-4 test was almost 7,000 lbs. The difference was believed to be caused by the complexity of the real-life test setup. In the LPILE Plus model, the H-pile was embedded in an ideally uniform 350 soil; while in the physical test the 350 soil only existed in a drill hole with a diameter of 36 in., as shown in the left-oriented diagram of Figure 5.2. Also there was a concrete slab nearby with a thickness of 24 in. Both the soil around the drill hole and the nearby thick concrete slab confined the 350 soil and affected its performance. At the beginning of the post rotation, the 350 soil was less affected by the surrounding confinement. The performance at the early stage was, for the most part, accurately captured by LPILE Plus simulation; the confinement effect caught up later on and resulted in large ultimate strength, as shown in Figure 5.4. Thus, the simulation result from LPILE Plus was proven to be reliable and the K value of 900 lb/in³ was used for 350 soil analysis herein.

$$P = (g)(b)(L*L*L)(Kp)/(2e+2L) = (0.08) (5.68) (40*40*40) (4.6)/(2(25+40)) = 1029 \text{ lbs.} \quad \text{Eq. 5}$$

Where

P: Ultimate Pile Load

g: Soil Density

b: Pile width

L: Pile Embedment Length

Kp: Coefficient of Passive Soil Pressure

e: Load Height from Ground Line

5.4 LPILE Plus Analysis of Concrete Shaft Anchor Design

This evaluation was conducted under the worst case load, assuming the foundation was subjected to the impact of a 2270P pickup truck while the pretension was very high (-20 F). The lateral load resulting from this scenario is about 40 kips. Since the temperature and impact loads are approximately equal, this evaluation represents a factor of safety of about 2 in respect to either load independently.

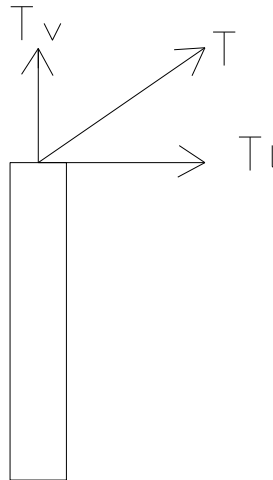


Figure 5.5 Illustration of External Force on Anchor Head

Head deflection is mainly caused by force in the lateral direction. In order to simplify the analysis, the baseline model for the LPILE analysis was set up as a concrete shaft embedded in soil with a lateral external force applied on the head of the concrete shaft at ground level, as shown in Figure 5.6.

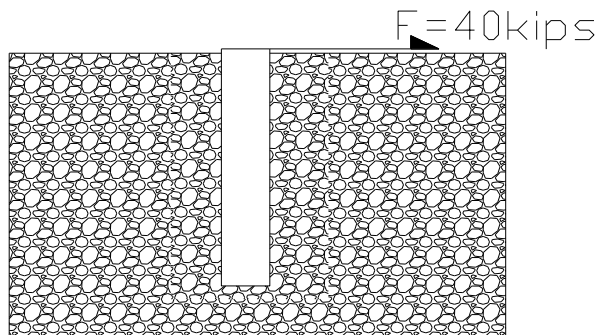


Figure 5.6 Illustration of LPILE Plus Model Setup

The boundary condition in the LPILE Plus model used type 1 (force and moment), as shown in Figure 5.7. The failure of a foundation was considered at the point when the pile was pulled out, or “plowed,” through the soil.

Three different soil conditions were investigated in the LPILE simulation: well graded crushed stone as defined in NCHRP Report 350, stiff clay, and sand. As drilled concrete piles

have become the foundation of choice with many of the Midwest Pooled Fund States this configuration was selected for evaluation. Three diameters (12, 18 and 24 in.) were evaluated at a variety of embedment depths. For a cylindrical concrete pile in the three soils analyzed herein, recommendations are based on acceptable deflection of the anchor as defined by the author (4 in.) and anticipated loads. Based on a particular state’s weather, soil conditions and post impact maintenance goals, the results and subsequent recommendations will be dramatically different.

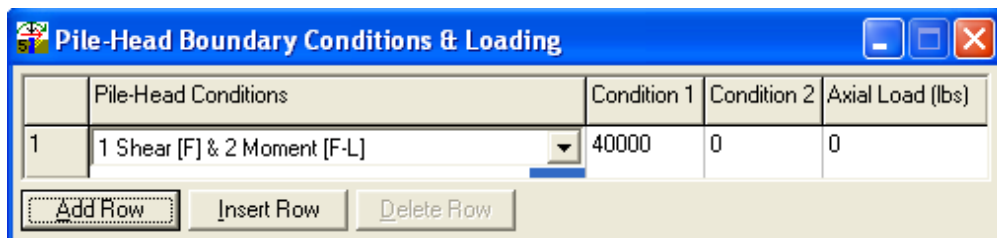


Figure 5.7 Boundary Condition Input in LPILE Plus

5.4.1 Anchor Deflection in 350 Soil

The 350 soil was simulated using the API Sand model embedded in LPILE Plus, using the input parameters determined from the validation of the NYBBT-4 static soil test, as shown in Figure 5.8. The performance of the concrete shaft anchor was investigated with variable diameters and embedment depths in NCHRP 350 Soil. The simulation results are plotted in Figure 5.9 and Figure 5.10.

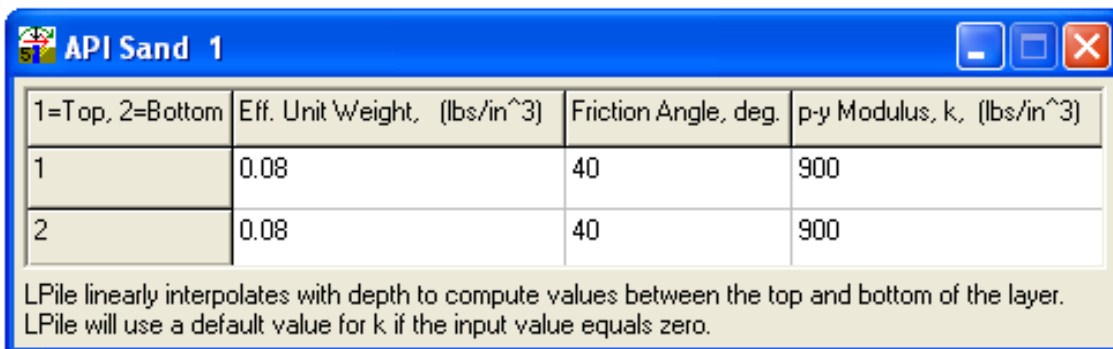


Figure 5.8 NCNRP 350 Soil Model Input Parameters in LPILE Plus

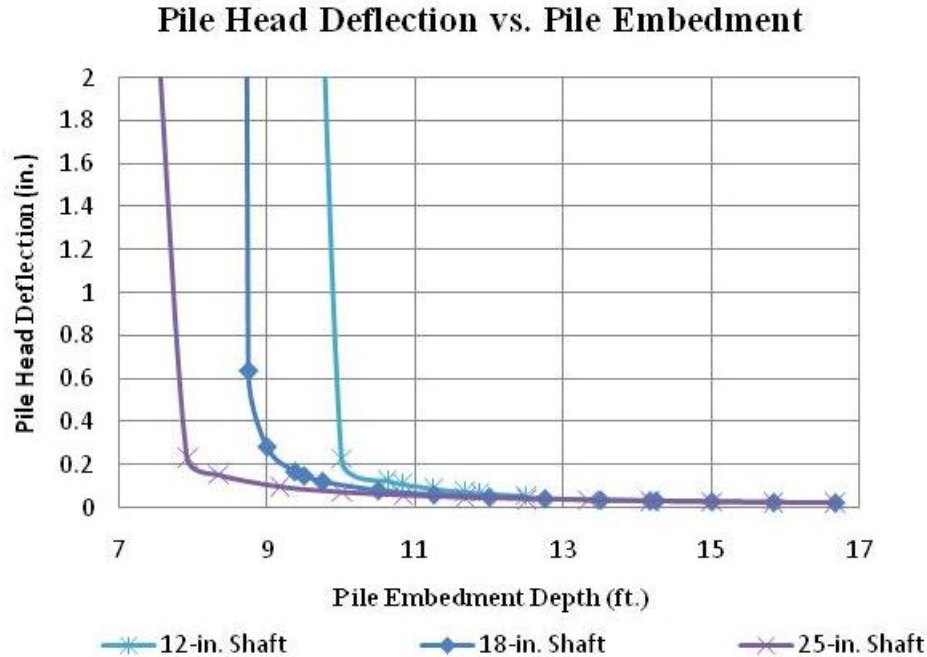


Figure 5.9 Concrete Shaft Head Deflection vs. Embedment Depth in NCHRP 350 Soil

As shown in Figure 5.9, the diameter of the pile clearly affected the pile’s failure embedment. To avoid being pulled out by the 40 kips lateral load, the shortest working pile length varied between 8 ft and 10 ft when the pile diameter was between 24 in and 12 in, as listed in Table 5.4.

Table 5.4 Failure Embedment Depths of Concrete Shaft in NCHRP 350 Soil

Diameter Size (in.)	Failure Depth (ft.)
24	7.9
18	8.9
12	10

Meanwhile, the pile’s embedment depth also effects its head deflection. Generally, the deeper the embedment is, the less deflection the pile head will have. As is clearly shown in Figure 5.10, in this particular case (under 40 kips lateral load) the pile’s performance improves

with the growth of the pile length. However, the growth of pile embedment will encounter a critical depth, and the effect of the pile length on head deflection diminishes beyond this point. Out of consideration for cost, the pile length is not recommended to be deeper than this critical value. For a 12 in. diameter pile, the pile's critical length in NCHRP 350 soil is around 14 ft, while the critical depths for the 18 in. and 24 in. diameter piles are both around 12 ft. The proper pile length should be chosen between the range of the pile's failure embedment and critical embedment.

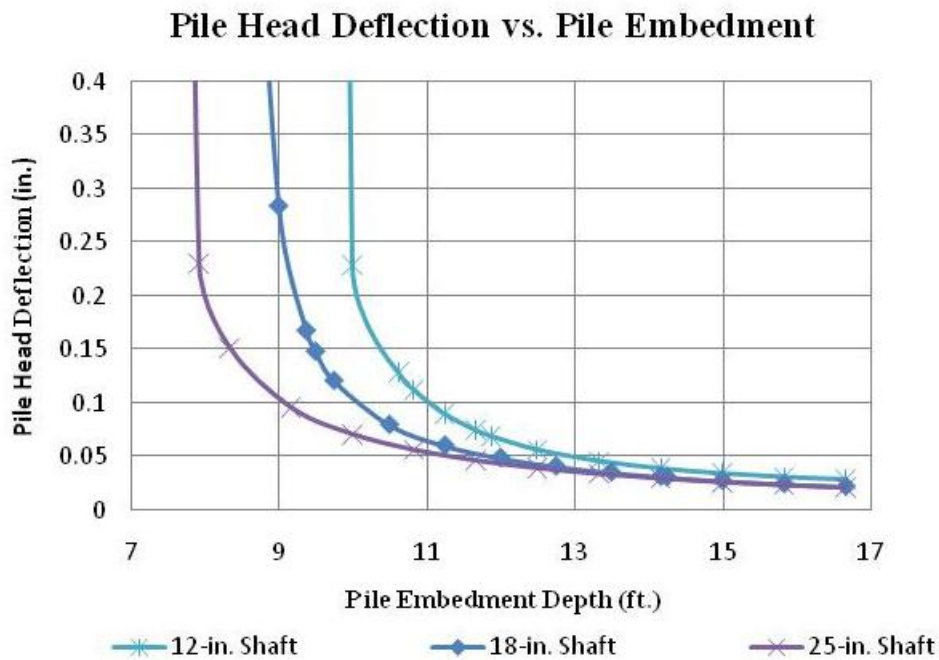


Figure 5.10 Close-Up View of Concrete Shaft Head Deflection vs. Embedment Depth in NCHRP 350 Soil

5.4.2 Anchor Deflection in Stiff Clay Soil

The stiff clay was modeled using the model Stiff Clay w/o Free Water in LPILE Plus, and its input parameters are shown in Figure 5.11. A 40 kip lateral load was applied to the concrete head, and the head deflections of three different diameter piles are plotted with respect to their embedment depths in Figure 5.12.

As shown in Figure 5.12 and Table 5.5, the 12 in diameter pile failed when its embedment depth was less than 13.2 ft, while the 18 in diameter pile and 24 in diameter pile failed when the embedment was shorter than 10.8 ft and 9 ft respectively. Meanwhile, the pile’s performance did not significantly improve if the embedment exceeded a critical value. In stiff clay, the critical embedment for each size of concrete piles are listed in Table 5.6. For economic considerations, the pile’s lengths should not exceed the critical values.

1=Top, 2=Bottom	Eff. Unit Weight, (lbs/in ³)	Undrained Cohesion, c, (lbs/in ²)	Strain Factor, E50
1	0.069	10.42	0.005
2	0.069	10.42	0.005

LPile linearly interpolates with depth to compute values between the top and bottom of the layer.
 LPile will use default values for E50 if the input value equals zero.

Figure 5.11 Stiff Clay Soil Model Input Parameters in LPILE Plus

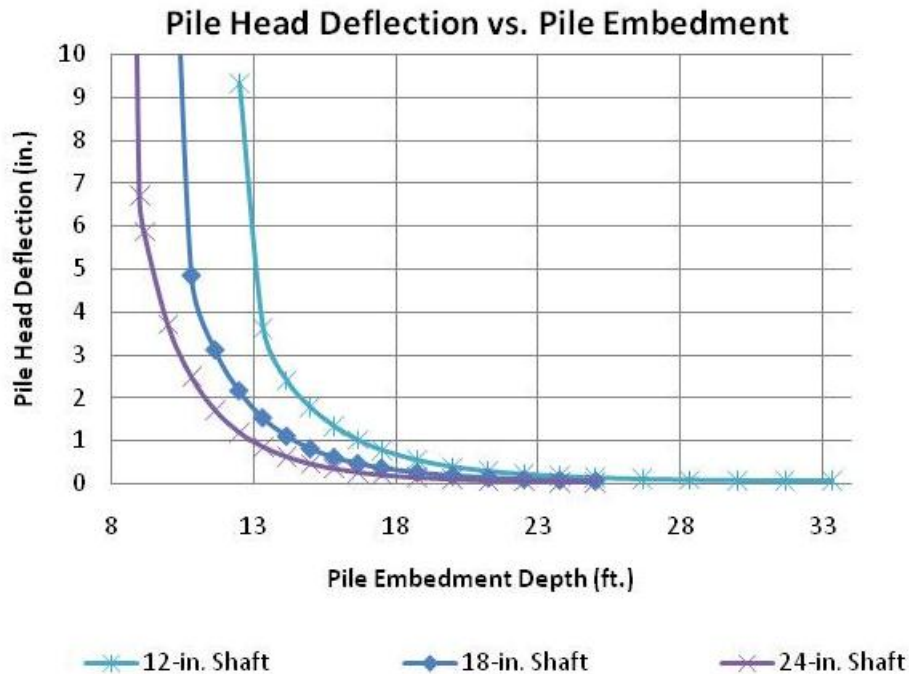


Figure 5.12 Concrete Shaft Head Deflection vs. Embedment Depth in Stiff Clay

Table 5.5 Failure Embedment Depths of Concrete Shaft in Stiff Clay

Diameter Size (in.)	Failure Depth (ft.)
24	9
18	10.8
12	13.2

Table 5.6 Critical Embedment Depths of Concrete Shaft in Stiff Clay

Diameter Size (in.)	Critical Depth (ft.)
24	17
18	19.2
12	22.5

5.4.3 Anchor Deflection in AASHTO A3 Sand

The AASHTO A3 sand was chosen to represent the extreme weak soil, and was modeled using API Sand in LPILE Plus. The input parameters of the sand are shown in Figure 5.13. A 40 kip lateral load was applied to the concrete head, and the head deflections of three different diameter piles are plotted with respect to their embedment depths in Figure 5.14.

As it shown in Figure 5.14 and Table 5.7, the 12 in. diameter pile failed when its embedment was less than 11.2 ft, while the 18 in. diameter pile and 24 in. diameter pile failed when the embedment was shorter than 12.5 ft and 13.4 ft, respectively. Meanwhile, the pile's performance did not significantly improve if the embedment went beyond a critical value. In stiff clay, the critical embedment for each concrete pile is listed in Table 5.8. For economical considerations, the pile lengths should not exceed the critical values.

1=Top, 2=Bottom	Eff. Unit Weight, (lbs/in ³)	Friction Angle, deg.	p-y Modulus, k, (lbs/in ³)
1	0.064	34	90
2	0.064	34	90

LPIle linearly interpolates with depth to compute values between the top and bottom of the layer.
 LPIle will use a default value for k if the input value equals zero.

Figure 5.13 Granular Rock Model Input Parameters in LPILE Plus

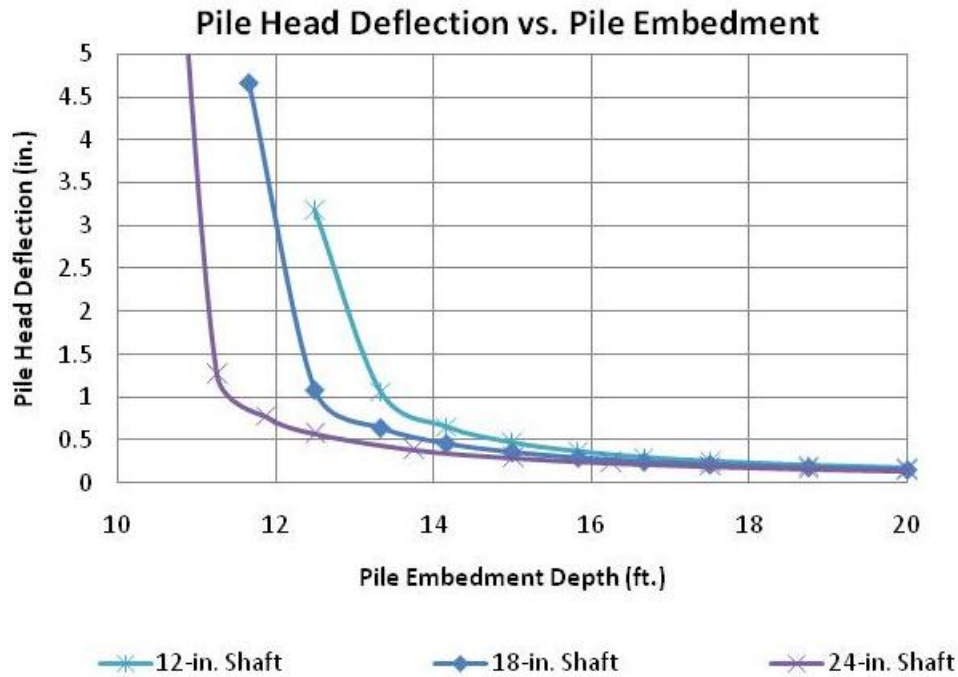


Figure 5.14 Concrete Shaft Head Deflection vs. Embedment Depth in Granular Rock

Table 5.7 Failure Embedment Depths of Concrete Shaft in Granular Rock

Diameter Size (in.)	Failure Depth (ft.)
24	11.2
18	12.5
12	13.4

Table 5.8 Critical Embedment Depths of Concrete Shaft in Granular Rock

Diameter Size (in.)	Critical Depth (ft.)
24	17.5
18	18
12	18.5

5.5 Summary and Conclusion

Based on the evaluation of previous MwRSF bogie tests, the concrete shaft was determined to be an appropriate choice for the high tension cable anchor design. However, the performance of the concrete shaft depends on its diameter, embedment depth, and the surrounding soil type. In order to determine the appropriate concrete shaft design that would assure the high tension cable's performance while at the same time maintaining reasonable initial costs, LPILE Plus was used. Pile's head deflections under external load were investigated in different soil types.

After obtaining the thermal load and thermal deflection of cable from analytical calculations, the tension-deflection curves of cable under different temperatures was plotted using linear elastic assumption, as shown in Figure 3.4. By overlapping the cable tension-deflection curves with the anchor load-deflections curves from physical tests and simulations, the actual tension in a cable anchored by a certain type of anchorage can be determined by locating the intersection of the two curves. Figures 4.1 and 4.2 are the plots of actual tensions under different temperatures in a cable anchored by the H-pile and concrete shaft used in the bogie tests CA-1 and CA-3. LPILE Plus simulation curves were also plotted in addition to the bogie test curves to serve as a reference.

Chapter 6 Conclusions

Based on a particular state's weather, soil conditions and post impact maintenance goals, the results and subsequent recommendations will be dramatically different. Therefore the results in Table 6.1 are only presented as a methodology to approach design and not specific design embedment for a given location.

Because high tension cable foundations are subjected to static loads that may induce deflection and negatively impact the performance of the system, it is necessary to take steps beyond the evaluation of full-scale crash testing to evaluate the efficacy of the anchor design. As shown herein, consideration of weather, soil, and system details all serve a critical role in the design of an appropriate foundation. Based on a design load selected from initial cable tension, potential temperature induced and impact loads, an LPILE analysis using appropriate soil conditions yielded an effective evaluation of the required foundation diameter and embedment depth. This approach is certainly applicable for a range of different foundation configurations and cable geometries.

In many cases the cost of incrementally increasing embedment depth to account for changing soil conditions may not be cost effective, as the engineering cost of evaluating specific site conditions will often exceed the cost of the foundation depth. Many states have selected a particular foundation design based on principals discussed herein for a "worst case" scenario and applied this design universally across all sites. These design decisions will of course be based on the breadth of soil conditions that are anticipated.

Table 6.1 Recommended Embedment for Cylindrical Concrete Foundation

	12 in. Diameter Shaft	18 in. Diameter Shaft	24 in. Diameter Shaft
	Minimum Embedment Depth (ft)	Minimum Embedment Depth (ft)	Minimum Embedment Depth (ft)
350 Soil	10	9	8
Stiff Clay	13	11	9
Sand	13.5	12.5	11.5

References

1. Zhu, L. and J.R. Rohde. *Development of Guidelines for Anchor Design for High tension Cable Guardrails*. Submitted to the 88th Annual Meeting of the Transportation Research Board, Paper No. 10-3391. Midwest Roadside Safety Facility, Lincoln, Nebraska, November 15, 2009.
2. Reese, L. C. and S.T. Wang. “Verification of Computer Program LPILE as A Valid Tool For Design of A Single Pile Under Lateral Loading.” August 2006.
3. Broms, B.B. “Lateral Resistance of Piles in Cohesive Soils.” *Journal of Soil Mechanics and Foundations Division A.S.C.E.* 90.SM2 (March 1964): 237-263

END OF DOCUMENT